N° d'ordre

UNIVERSITE KASDI MERBAH OUARGLA
FACLUTE DES MATHEMATIQUES
ET DES SCIENCES DE LA MATIERE
DEPARTEMENT DE PHYSIQUE

Mémoire

MASTER ACADEMIQUE

Domaine : Sciences de la Matière
Filière : Physique
Spécialité : Physique des Rayonnements

Présenté par : **BAHAZ Ahlam**

Thème :

Calculation of concentrations of neutral particles in SiH_4/O_2 gas mixture in Inductively Coupled Plasma (ICP).

Soutenu publiquement:
Le : 22 / 06 / 2021
Devant le jury composé de:

Dr LEMKEDDEM Soumaya	MCB	Président	UKM OUARGLA
Dr BALLAH Zakia	MCB	Examinateur	UKM OUARGLA
Dr GADOUM Abdelatif	MCB	Co-Encadreur	UKM OUARGLA
Pr KHELFAOUI Fethi	Prof.	Rapporteur	UKM OUARGLA

Année Universitaire : 2020/2021

Dedication

To my parents

To my family

To my friends

To my colleagues

Acknowledgements

Firstly thanks to all Allah. This work could never has been completed without the support of my supervisor Pr KHELFAOUI Fethi. I appreciate his valuable advices, instructions and suggestions on various drafts of this work and his continuous patience and supervisor assistance Dr GADOUM Abdelatif. I also thank the board of examiners: President Dr LEMKEDDEM Soumaya and Examiner, Dr BALLAH Zakia for their acceptance to judge this work.

I am thankful to my colleagues of our LPRPS laboratory PhD students KHELEF Nour, KEBAILI Hadja OumKeltoum and BERGOUG Sadia; they have helped me immensely in several occasions. besides my friends MAYOU Messouda and CHAIB Wafa who incouraged and helped me continuously.

Index of contents

List of figures

List of tables

General introduction

General introduction

In our days the use of thin films has widely increased in different fields like: the fabrication of solar cells and the microelectronics industry for the fabrication of electronic devices. Thin films deposition can be obtained by:

- Chemical phase (Chemical Vapor Deposition CVD);

- Physical phase (Physical Vapor Deposition PVD).

One of the most known and used techniques in the industry field is a method of chemical vapor deposition CVD of thins films deposition and precisely is Inductively Coupled Plasma (ICP); we will summarize our study on.

The purpose of our work is to calculate the concentration of different particles with gas mixture SiH_4/O_2 in reactor of one dimension and stationary system in ICP. We use data of the work of S. Tinck and A. Bogaerts [1] where they studied the properties of a SiH_4/O_2/Ar in ICP and how it interacts with a silicon substrate (wafer). In our work, we neglected the Argon gas.

Our work is of three chapters as follows:

In the first chapter we present plasma generalities (definitions and physical parameters), a sight of Inductively Coupled Plasma (ICP), meaning and principle also types of ICP reactors; we also present the principle equations of the fluid model.

In the second chapter, we mention the physical phenomena of the reactor. We choice the first equation of the fluid model, the equation of continuity, to resolve the problem. We present most important steps of the mathematical and numerical processing used to calculate the concentrations of different neutral species (molecules and radicals) in the reactor.

The third chapter is a presentation of the results of the calculation using numerical calculation program in Fortran77 language. Results of the calculation are discussed.

.

Chapter I: Generalities on Inductively Coupled Plasma (ICP)

Chapter I:
Generalities on Inductively Coupled Plasma (ICP)

1.1. Introduction

In this chapter, we present an introduction to plasma physics for thin film deposition. We present the technique and some types of reactor for the deposition of the inductively coupled plasma (ICP). The fluid model equations can be very useful for the study of these plasmas.

I.2. Plasmas physics

I.2.1. The definition of Plasma

The plasma is known as the fourth state of material, consists a gas of charged particles at very high temperature, in which the potential energy of a typical particle due to its nearest neighbor is much smaller than its kinetic energy. The word plasma comes from the Greek plásma, which means something formed or modeled. This latter was introduced by Langmuir and Tonks at the beginning of the 20^{th} century to describe ionized gases, we should also consider that the plasma comprises equal numbers of singly charged ions (+e) and electrons (-e) [2].

I.2.2. The properties of plasma

More than 99% of the known universe is in the plasma state, for example: stars, nebulae, auroras or lightning, beside the artificial plasma like inductively coupled plasma which our study is about These kinds of plasmas have very different properties and as a first classification can be made as a function of the charges density and electron temperature.

Plasmas can be classified by the degree of temperature and the density of electrons, for example : interstellar plasmas have a very low density (approximately 10^6 electrons$\cdot m^{-3}$) and low temperature (below 10^3K), on

the opposite side star cores are both high temperature (approximately 10^7 K) high density (above 10^{28} electrons·m^{-3}) , while the artificial plasma are usually low temperature (except for fusion plasma) , but at high densities from around 10^{16} electrons per m^3 for glow discharges up to10^{24} electrons per m^3 for "thermal" plasmas like electrical arcs [3].

I.2.3. Cold plasma

Cold Plasma is a gas weakly ionized, it consists of positive and negative charges, for example: electrons and negative ions beside neutral particles, these latter are characterized by several parameters: pressure, temperature and also physical proprieties [4].

I.2.4. Plasma frequency

Plasma frequency is a frequency related to vibrational columbic movement charged particles inside the plasma due to displacement off balance position which was discovered by the Dutch physical Franck Michel in 1926 [5].

$$w_{\mathrm{pe}} = \frac{\sqrt{n_{e0}p2}}{\sqrt{me\varepsilon_0}} \quad \text{(I.1)}$$

$$w_{pe} = \sqrt{\left(\frac{N_{e,i}}{m_{e,i}\varepsilon_0} q_{e,i}^2\right)} \quad \text{(I.2)}$$

$$w_{pe}=5.64 * 10^4\sqrt{N_e(cm^{-3})} \quad \text{(I.3)}$$

$$w_{pe} = 0.02334 * Z^{\frac{3}{2}} * w_{pe}(rad.S^{-1}) \quad \text{(I.4)}$$

w_p: plasma frequency

q_i : ion charge

q_e : electron charge

$N_{e,i}$: initial electronic and ionic density before the perturbation occurs.

ε_0: the permittivity of free space.

m_e: electron mass.

Electronic plasma frequency.

$$f_e(HZ) = \frac{w_{pe}}{2\pi} \quad \text{(I.5)}$$

Ionized plasma frequency

$$f_i(HZ) = \frac{w_{pi}}{2\pi} \quad \text{(I.6)}$$

I.2.5. Debye's Length

Debye's Length is the distance over which significant charge (ions and electrons) separation occurs in a plasma .we can definite it as the measure of how far into the plasma the potential of an electrode is observed [6].

$$V_{Debye} : \frac{q_j}{4\pi\varepsilon_0 r}\ exp\left(-\frac{r}{\lambda_D}\right) \quad \text{(I.7)}$$

where λ_D represents Debye's length :

$$\lambda_D = \sqrt{\frac{\varepsilon_0\ k_B T}{q_e^2 N_e}} \quad \text{(I.8)}$$

Where:

ε_0: the permittivity of free space.

K_b: Boltzmann's constant.

q_e: the charge of electron.

N_e: is Density electronic

I.3. Thin films deposition

I.3.1. Definition of thin film

A thin film is a wafer of a matter has a thickness of rate (µm to nm), deposited on the substrate in order to provide it with specific chemical or physical properties. It's also an organization of material elements in two dimensions where the third dimension is so small [7].

There are different techniques of thin films deposition. We can consider two main techniques as shown in the picture in below (Figure I.1).

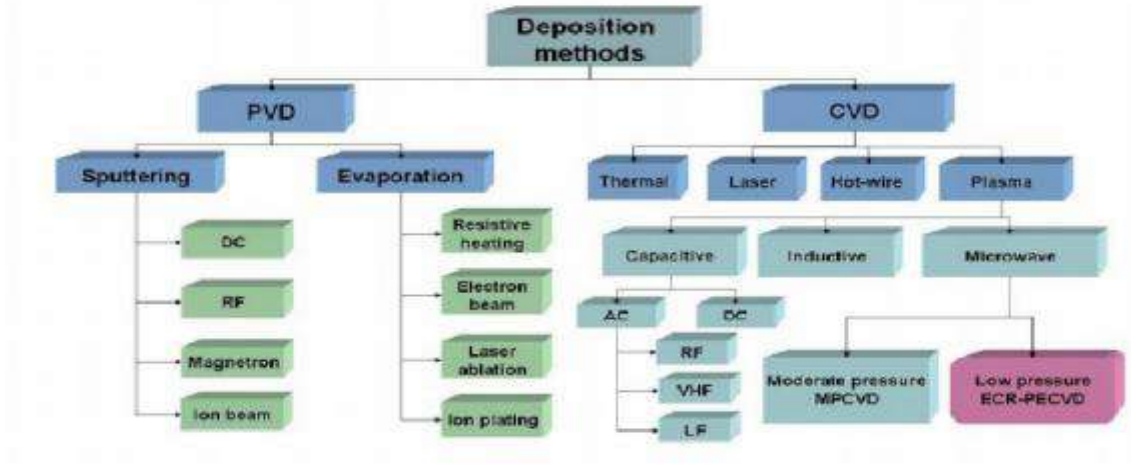

Figure I.1: Techniques used for thin films deposition [8].

I.3.2. Physical Vapor Deposition (PVD) [9]

Physical Vapor Deposition is a method of thin films deposition depends on physical phenomena the deposition is achieved by condensation phenomena under low pressure for material vapor and it is classified according to material vapor and the condensation vapor techniques which are:

- Thermal evaporation under vacuum.

- Cathodic spray.

- Ionized sedimentation.

I.3.4. Chemical Vapor Deposition (CVD)

Chemical Vapor Deposition is a method of thin films deposition depends on chemical reactions with gases. The gas is injected inside the reactor. The gas composition dissociates and interacts with the substrate surface at a certain conditions (temperature and pressure) which are proportional with used deposition technique [10].

There are so many types of CVD deposition we mention:

- CVD deposition at high pressure HPCVD.
- CVD deposition under low pressure LPCVD.
- CVD deposition at atmospheric pressure PACVD.
- CVD deposition with plasma PECVD.
- CVD deposition using Laser LCVD.
- CVD deposition using photons photo-CVD.
- CVD deposition by hot wire HWCVD.

I.4. The Inductive Coupled Plasma (ICP

I.4.1. The concept of ICP

The concept of ICP systems generating is reduced from Faraday's law,owing into an antenna coil induces fl∂B/∂t. An RF current -×E=∇ magnetic field varies with time. This latter produces an induction field, which generates and sustains the plasma. This system can be thought of as a transformer circuit where the antenna coil acts as the primary circuit, while the plasma forms the secondary circuit with a single circular loop. As is exhibited in figure I 2 [11].

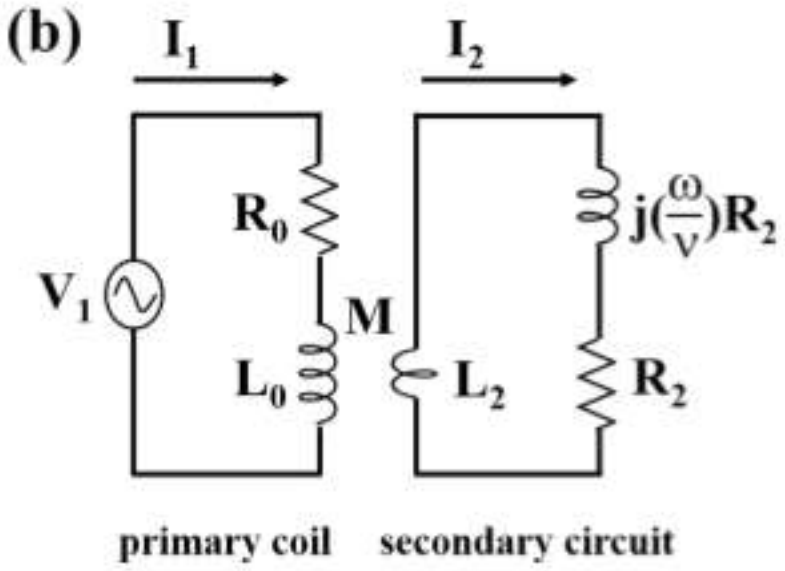

Figure I.2: ICP generation.

I.4.2. Principle of ICP

A Radio Frequency (RF) current flowing in a coil creates an electromagnetic field which plays an important role in ICP. Figure I.2 shows the RF magnetic field (B-field) and RF electric field (E-field) created inside the plasma chamber by applying RF power to the planar coil through the dielectric window. The main energy absorption mechanism in ICP is Joule heating, where the E-field accelerates the electrons these latter collide numerous times with other particles. The voltage drop per unit length equals the electric field E, and the electron drift velocity equals $\mu_e E$, so the Joule heating power Pj is expressed as follows [12]:

$$P_{j=en_e \mu_e E^2} \quad \text{(I.9)}$$

Where:

E: is the electron charge.

$n_{e:}$ is the electron density.

$\mu_{e:}$ is electron mobility.

Another energy absorption mechanism in ICP is considered important as well because HDP (high density plasma) can be maintained at very low collisionless pressure known as Stochastic heating by anomalous skin effects. This latter means: heating without collision. If the mean free path of an electron is sufficiently larger than the skin depth of the electromagnetic field, then electrons penetrating into the skin region δ depth under the dielectric window, can receive energy from the electromagnetic field. When the excitation angular frequency ω is sufficiently larger than the elastic collision frequency ν, skin depth δ is written as:

$$\delta = \frac{C}{\omega_{pe}} \qquad \text{(I.10)}$$

Where:

C: is speed of light

W_{ipe}: electron plasma angular frequency

Figure I.3 shows the RF magnetic field (B-field) and RF electric field (E-field) created inside the plasma chamber [12].

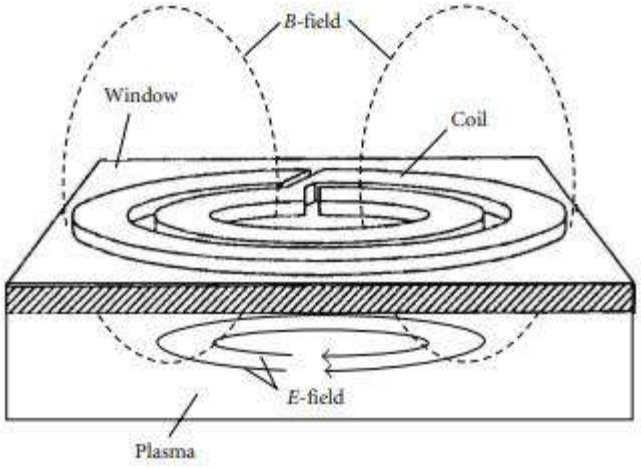

Figure I.3: RF magnetic field (B-field) and RF electric field (E-field) created inside a plasma chamber [12].

In processing, plasma δ can be roughly estimated in the order of mm to cm. Equation (10) is based on the hypothesis that electrons have very small energy and create no thermal motion. If the collision frequency ν becomes so small at low pressure that ω and ν are much smaller than v/2δ, then the time scale of interaction between electrons and the electric field, while electrons are in the skin region becomes shorter than that of electromagnetic field fluctuation and collisions. As a result, electrons accelerating inside the skin region can return to bulk plasma without losing their kinetic energy and thus contribute to ionization.

I.4.3. ICP reactors

Here we take 3 types of ICP reactors:

Type 1:

In the first type we obtain a full cylindrical reactor by rotating the plane around the left axis. The reactor has two coils first one is a planar on the top of the chamber and second one is cylindrical coil surrounding the chamber. The silicon substrate is located at the bottom of the chamber which is 300mm wafer placed on the top of the substrate electrode [1].

Operating conditions used for the experiment:

-13.56 MHz radio frequency applied both at the coil and the substrate.

-10m Torr total gas pressure.

-500 sccm total gas flow rate.

-60 ^{0}C substrate and wall temperature.

-4400 W coil power (1300W comes from the top coil and 3500W substrate bias power.

Figure I.4 shows Two-dimensional reactor geometry defined. The left axis is the symmetry axis of the cylindrically symmetrical reactor [1].

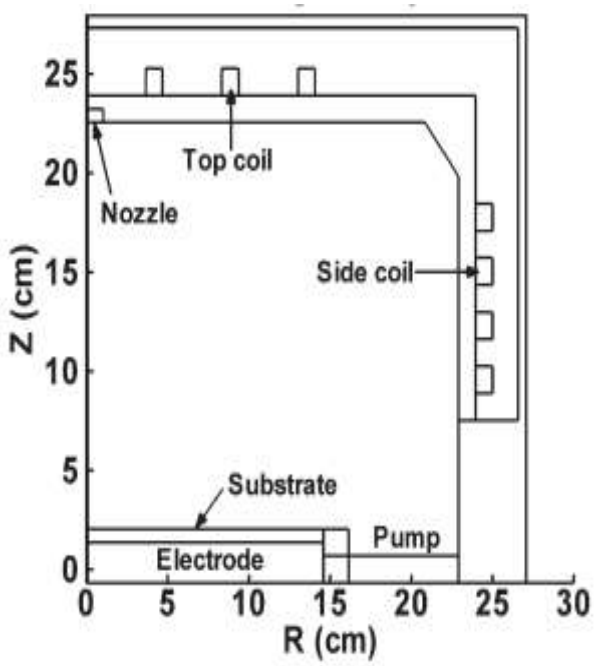

Figure I.4: Two-dimensional reactor geometry [1].

Type 2 :

The inductively coupled plasma (ICP) reactor shown in Figure I.6 is used for the deposition of a-Si:H and nc-Si:H films.

Operating conditions used for the experiment:

-13.56 MHz radio frequency applied between the center and the edge of spiral coil through a matching network which maintains the plasma below the quartz window.

-A turbo-molecular pump with a pumping speed of 1000 l/s sustains a base pressure of $4*10^{-27}$ Torr. A throttle valve enables pressure regulation independent of the gas flow. Gas flow rates are controlled by mass flow controllers and pack-less meter valves. SiH_4 (1% in Ar) is introduced into the chamber by a gas injection ring located just above the substrate electrode. The temperature of the stainless steel substrate electrode is regulated by a feedback controller with a 300 W ring heater and a thermocouple located just below the sample position. Substrate temperature may be maintained from (25 - 500 °C).

-Argon and H_2 are fed into the chamber through an upper injection ring in the region of intense plasma.

Figure I.5 shows a schematic of the Inductively Coupled Plasma reactor and the in situ total internal reflection Fourier transform infrared spectroscopy setup [13].

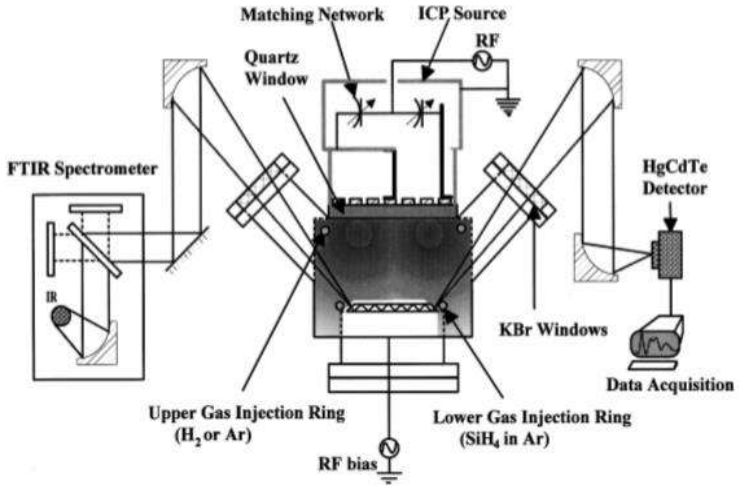

Figure I.5: Schematic of the Inductively Coupled Plasma reactor and the in situ total internal reflection Fourier transform infrared spectroscopy setup [13].

Type 3:

The figure I.6 shows an ICP plasma reactor and the LPCVD/MOCVD rotating disc reactor [14].

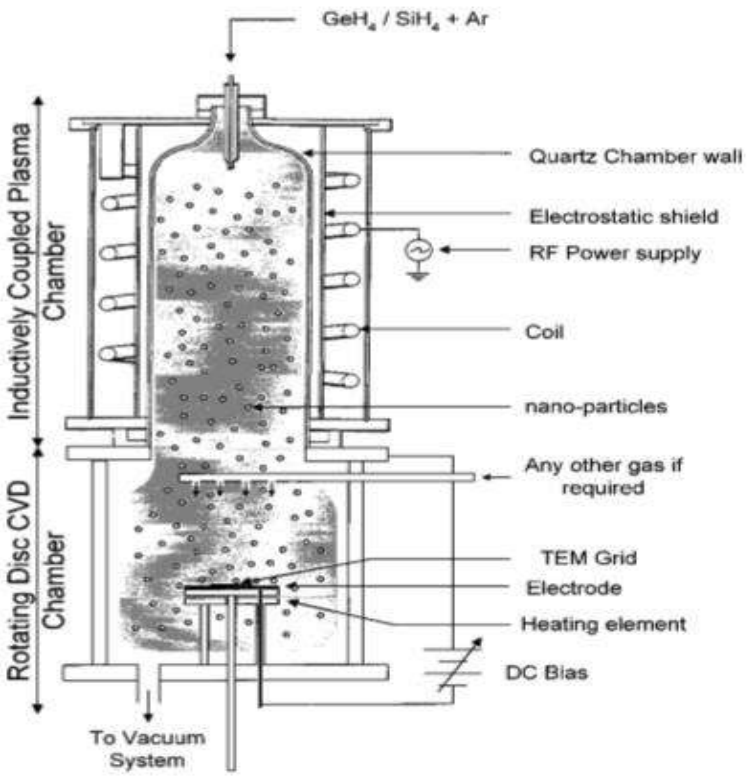

Figure I 6: ICP plasma reactor and the LPCVD/MOCVD rotating disc reactor [14].

This type of reactor consists of a helical conducting coil placed between a cylindrical outer shield and an inner quartz tube to confine the plasma. In addition, the system is electrostatically shielded by placing a conducting sheet with longitudinal slots (split Faraday shield) in-between the helical coil and the inner quartz tube. This shield prevents any capacitive excitation of the plasma. The water cooled inductive coil is driven by a 1200.W.There are gas inlets into the plasma reactor as well as into the rotating disk reactor. The plasma chamber is placed on top of a rotating disk low pressure chemical vapor deposition/metal organic chemical vapor deposition (LPCVD/MOCVD) reactor. This setup was used so that particles generated in the plasma chamber could be incorporated into a growing film in the LPCVD chamber if desired. The rotating disk LPCVD reactor consists of a horizontally placed wafer

succeptor (about 15 cm from the bottom of the plasma chamber) which can be rotated at high speeds a. a resistive heater is placed just below the succeptor. The plasma power varies from 300 to 900 W.

I.4.4. Operating conditions used for the experiment

-13.56 MHz radio-frequency power supply through a matching network for efficient power transfer.

-The plasma chamber is approximately 20 cm in diameter and 20 cm long.

-The system is pumped down to a pressure of 30–50 mTorr.

-Plasma enhanced chemical vapor deposition (PECVD) is an appropriate process for microtrench (gap) filling during shallow trench isolation (STI) in semiconductor device processing as applied in the microelectronics industry [14].

I.5. The movement of charged particle in magnetic field:

$$\frac{m\overrightarrow{dv}}{dt} = q\vec{E} + q\vec{v} \times \vec{B} - mv\vartheta \qquad \text{(I.11)}$$

Case of:

$\vec{E} = E_r\overrightarrow{e_r}$ and $\vec{B} = B_z\overrightarrow{e_z}$

$$\vec{v} = qE_r\left(\frac{(i\omega+\vartheta)}{(mi\omega+m\vartheta)^2+(qB_z)^2}\right)\overrightarrow{e_r} - \frac{q^2B_zE_r}{(mi\omega+m\vartheta)^2} - \frac{E_r}{B_z}\overrightarrow{e_\theta} + \frac{qE_r}{m(i\omega+\vartheta)} \qquad \text{(I.12)}$$

Case of:

$\vec{E} = E_r\overrightarrow{e_r}$. and $\vec{B} = B_r\overrightarrow{e_r}$

We have only:

$$\vec{v} = \frac{qE_r}{m(i\omega+\vartheta)}\overrightarrow{e_r} \qquad \text{(I.13)}$$

I.6. The fluid model

The fluid model enables us from determining the medium average of physical quantities like: electrons density, ions density and neutral particles density etc. this model is a set of differential equations of partial derivations that are defined with the third moments of the Boltzmann equation, where density is represented by the continuity equation, and these differential equations can be resolved with a couple of methods for example: finite differences method or finite elements also finite volumes [9].

There are three principle equations of fluid model [15]: the continuity equation, the momentum equation and the energy equation. For calculation applications, we have to use additional equations. We can choose the equations of electromagnetism. We have opted for the equation of Poisson; it is the first equation of Maxwell's equations.

I.6.1. The continuity equation

$$\frac{\partial n_{e,i,n}}{\partial t}+\nabla \boldsymbol{J}_{e,i,n} = S_{e,i,n} \qquad \text{(I.14)}$$

$$J_{e,i,n} = -\mathrm{D_{e,i,n}}\nabla n_{e,i,n} \pm \mu_{e,i} n_{e,i} E \qquad \text{(I.15)}$$

Where:

$n_{e,i,n}$: is the species number density.

$J_{e,i,n}$: current flux density of particles (electrons ions neutral particles).

$S_{e,i,n}$: the species source term.

$D_{e,i,n}$: diffusivity coefficient of the particles (electrons ions neutral particles).

$\mu_{e,i}$: mobility coefficient (convection velocity) of electrons ions and neutral particles, for this latter equals zero while for (+)signal for positive ions and (–) signal for negative ions.

E: the electric field.

k_B: Boltzmann constant.

q: the elementary charge.

T_e: electron temperature.

I.6.2. The momentum equation

$$\frac{\partial(mj)}{\partial t} + \nabla.(nm\overline{\overline{VV}}) + \nabla.\mathrm{P} - nF = R_m \qquad \text{(I.16)}$$

N: particles density.

υ: particle's velocity.

P: pressure.

F: external force applied by electrical and magnetic field or others.

R_m: lost momentum.

I.6.3. The energy equation

$$\frac{d(n\varepsilon)}{dt} + \nabla.q - nF.V = R_{ev}. \qquad \text{(I.17)}$$

Where $q = j\varepsilon + \mathrm{V}.\mathrm{P}$ total flux vector.

R_{ev}: loss energy rate.

ε: thermal energy.

I.6.4. The Poisson's Equation

Equation of Poisson is the first equation of Maxwell's equations which expresses the variation of the electric field in terms of the charges existing in space. It can be written by the following expression:

$$\nabla E = \frac{n_e\,(-e)+n_{ion}(+e)}{\varepsilon_0} \qquad \text{(I.18)}$$

Where:

n_e: electrons density.

n_{ion}: ions density.

While the electric potential is expressed by: $\vec{E} = -\overrightarrow{grad}V$.

Chapter II: Modelization of calculation of neutral particles concentration in ICP reactor

Chapter II: Modelization of calculation of neutral particles concentration in ICP reactor

II.1. Introduction

In this chapter we interest in study of SiH_4/O_2 gas mixture of Inductively Coupled Plasma (ICP) reactor. We present a model for calculation of concentration of different neutral particles. The dimensions of the reactor and the parameters of the experiment are those of the work of S. Tinck and A. Bogaerts (2012) [1]. In their work, they studied the properties of the gas mixture $SiH_4/O_2/Ar$ for Inductively Coupled Plasma (ICP) and how it interacts with a silicon substrate (wafer).

II.2. Physical phenomenon

In order to estimate characteristics of SiH_4/O_2 mixture used in thin films deposition in an ICP reactor, we concentrate the study on the most 15 dominant particles inside the reactor beside the electrons. We propose a reactor in stationary system and we have to study properties along one dimension (the axis of the reactor).

We consider the conditions used by S. Tinck, and A. Bogaerts (2012) [1]:

-The reactor is 2D geometry. The cylindrical reactor is obtained by rotating the plane around the left axis. The reactor has two coils, a planar coil on top of the chamber and a cylindrical coil surrounding the chamber.

-13.56 MHz Radio Frequency applied between the center and the edge of spiral coil through a matching network which maintains the plasma below the quartz window.

-The applied pressure is 10 mTorr.

-The temperature of the wall and the substrate is: 60°C.

-The gas mixture injected inside the reactor is: 54% of SiH_4 and 46% of O_2.

-The chemical reactions inside the reactor are between different particles. The chosen natural particles (molecules and radicals) are: SiH_4, O_2, SiH_3, SiH_2, H_2, SiH_3O, H, SiH_2O, SiO, H_2O, SiH, SiO_2, OH, SiHO, O.

-Species Diffusion Coefficient is considered variable with position z.

-The figure (II.1) below shows a simplified geometry of the reactor.

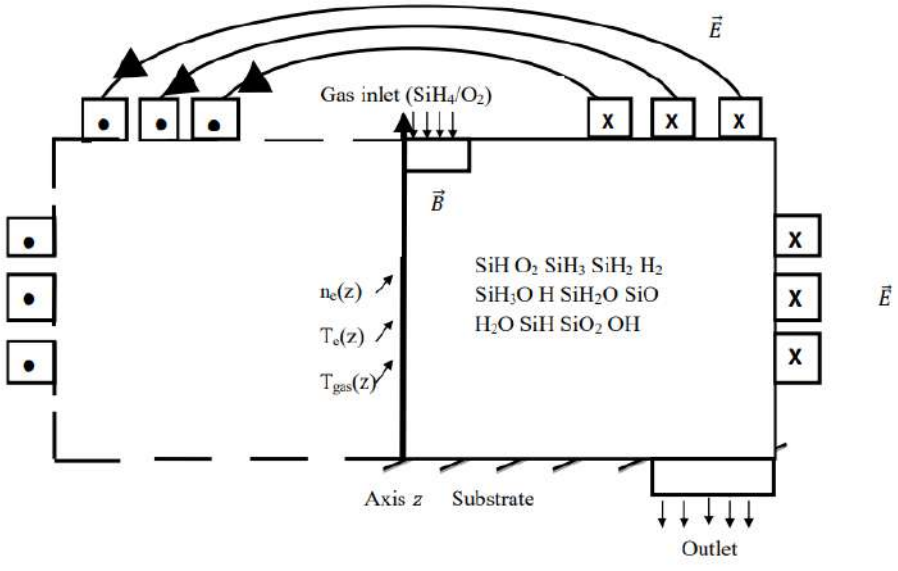

Figure II.1: Physical phenomenon.

II.3. Mathematical model

II.3.1. The continuity equation

The principal equation that is necessary to calculate concentration of neutral particles is the continuity equation **[**15**]:**

$$\frac{\partial C_k}{\partial t} + \vec{\nabla}(-D_k \nabla C_k) = S_k \qquad \text{(II.1)}$$

In a stationary states and for diffusion coefficient D_k which is slowly variable with space; we have for species k:

$$-D_k \nabla^2 C_k = S_k \qquad \text{(II.2)}$$

Or:

$$-D_k \frac{\partial^2}{\partial z^2} C_k = S_k \qquad \text{(II.3)}$$

Where:

S_k: source term [27]:

$$R_A = + \sum_{K_{reac}^{prod}} K_{reac(A',\,B')}^{cons} n_{A'}^{a'} n_{B'}^{b'} - \sum_{K_{reac}^{cons}} K_{reac(A,\,B)}^{cons} n_A^a n_B^b \qquad \text{(II.4)}$$

Rate constant: $K_{rea} = AT^B exp\left(-\frac{E_{act}}{k_B T}\right)$ (II.5)

With A, B and E_{act} constants related to the chemical reactions,

E_{act}: activation energy.

k_B: Boltzmann's constant.

T: gas temperature.

C_k: concentration of species k.

C_i, C_j : concentrations of species i and j respectively.

D_k: Diffusion coefficients of species k.

II.3.2. Chemical reactions of particles in the reactor

Table II.1 presents chemical reaction and their rate constants used in our model. The number of equations is 38. The different values of the constants were taken from:

- Some scientific articles (examples: Gorbachev [17], Kushner [18], Kushner [19], Bleecker et al.);

- Website UMIST astrochemistry.net: http://udfa.ajmarkwick.net/index.php [20].

- NIST website of the American Standards office, where there is data relating to chemical reactions of several gas mixtures: http://kinetics.nist.gov/kinetics/index.jsp [21].

Table II.1: Chemical reactions and Rate constants.

N°	Chemical reactions	Rate constant K_{reac}(cm^3/particle s)	ref
01	$SiH_4 + e \rightarrow SiH_3 + H + e$	$K_1=3\times10^{-11}$	[17]
02	$SiH_4 + e \rightarrow SiH_2 + H + H + e$	$K_2=1.5\times10^{-10}$	[17]
3	$SiH_4 + e \rightarrow SiH + H_2 + H + e$	$K_3=9.34\times10^{-12}$	[17]
4	$SiH_4 + H \rightarrow SiH_3 + H_2$	$K_4= K_4=7.49\times10^{-11}\times\exp(-\frac{13.39\times10^3}{(R\times T_{gas})})$ ga	[21]
5	$SiH_3 + H \rightarrow SiH_2 + H_2$	$K_5=2.67\times10^{-10}\left(\frac{T_{gas}}{298}\right)^{0.05}\exp(\frac{-640}{R\times T_{gas}})$	[21]
6	$SiH_3 + SiH_3 \rightarrow SiH_2 + SiH_4$	$K_6=2.99\times10^{-11}$	[21]
7	$SiH_2 + H_2 \rightarrow SiH_4$	$K_7=3.2\times10^{-12}$	[21]
8	$SiH_2 + H \rightarrow SiH + H_2$	$K_8=3.34\times10^{-11}\times\left(\frac{T_{gas}}{298}\right)^{1.82}\exp(\frac{-830}{R\times T_{gas}})$	[21]

9	$SiH_2 + H \rightarrow SiH_3$	$K_9=4.71\times10^{-10}\times\left(\frac{T_{gas}}{298}\right)^{0.47}\exp(\frac{-700}{R\times T_{gas}})$	[21]
10	$SiH + H_2 \rightarrow SiH_3$	$K_{10}=1.2\times10^{-12}$	[21]
11	$SiH + SiH_4 \rightarrow SiH_2 + SiH_3$	$K_{11}=5\times10^{-11}$	[21]
12	$O+OH \rightarrow H+O_2$	$K_{12}=3.5\times10^{-11}$	[21]
13	$OH+H_2 \rightarrow H_2O + H$	$K_{13}=6.7\times10^{-15}$	[21]
14	$OH+H \rightarrow O + H_2$	$K_{14}=6.89\times10^{-14}\times\left(\frac{T_{gas}}{298}\right)^{2.8}\exp(\frac{-16.21}{R\times T_{gas}})$	[21]
15	$O+H_2 \rightarrow OH + H$	$K_{15}=9\times10^{-18}$	[21]
16	$SiH_4 + O \rightarrow SiH_3 + OH$	$K_{16}=3.5\times 10^{-13}$	[21]
17	$SiH_4 + OH \rightarrow SiH_3 + H_2O$	$K_{17}=1.44\times 10^{-11}\times \exp(\frac{-400}{R\times T_{gas}})$	[21]
18	$SiH_4 + O_2 \rightarrow SiH_3O + OH$	$K_{18}=3\times10^{-12}$	[19]
19	$SiH_3 + O \rightarrow SiH_2O + H$	$K_{19}=2.16\times10^{-10}\times \exp(\frac{-1000}{R\times T_{gas}})$	[19]
20	$SiH_3 + OH \rightarrow SiH_2O + H_2$	$K_{20}=8.31\times10^{-12}$	[19]
21	$SiH_3 + O_2 \rightarrow SiH_2O + OH$	$K_{21}=6.3\times10^{-12}$	[19]
22	$SiH_3 + O_2 \rightarrow SiH_3O + O$	$K_{22}=6.3\times10^{-12}$	[19]
23	$SiH_2 + O_2 \rightarrow SiH_2O + O$	$K_{23}=3.75\times10^{-12}$	[19]
24	$SiH_2 + O_2 \rightarrow SiHO + OH$	$K_{24}=3.75\times10^{-12}$	[19]
25	$SiH + O_2 \rightarrow SiO + OH$	$K_{25}=8.5\times10^{-11}$	[21]
26	$SiH + O_2 \rightarrow SiO_2 + H$	$K_{26}=8.5\times10^{-11}$	[19]
27	$SiH_3O + O \rightarrow SiH_2O + OH$	$K_{27}=10^{-12}$	[19]

28	$SiH_3O + OH \rightarrow SiH_2O + H_2O$	$K_{28}=10^{-12}$	[19]
29	$SiH_2O + H \rightarrow SiHO + H_2$	$K_{29}=5.48\times10^{-10}\times\exp(\frac{-5276.4}{R\times T_{gas}})$	[19]
30	$SiH_2O + O \rightarrow SiHO + OH$	$K_{30}=2.99\times10^{-11}\times\exp(\frac{-1547.7}{R\times T_{gas}})$.	[19]
31	$SiH_2O + OH \rightarrow SiHO + H_2O$	$K_{31}=1.25\times10^{-11}\times\exp(\frac{-85.4}{R\times T_{gas}})$.	[19]
32	$SiHO + H \rightarrow SiO + H_2$	$K_{32}=3.32\times10^{-10}$	[19]
33	$SiHO + O \rightarrow SiO + OH$	$K_{33}=1.66\times10^{-10}$	[19]
34	$SiHO + OH \rightarrow SiO + H_2O$	$K_{34}=1.66\times10^{-10}$	[19]
35	$SiO + OH \rightarrow SiO_2 + H$	$K_{35}=6.65\times10^{-12}\times\exp(\frac{-2864.3}{R\times T_{gas}})$.	[19]
36	$SiO + O_2 \rightarrow SiO_2 + O$	$K_{36}=2.36\times10^{-10}\times\exp(\frac{-3266.3}{R\times T_{gas}})$	[19]
37	$H_2 + e \rightarrow H + H + e$	$K_{37}=3.22\times10^{-12}$	[20]
38	$O_2 + e \rightarrow O + O + e$	$K_{38}=6.86\times10^{-9}\times exp\left(-\frac{6.29}{T_e}\right)$.	[28]

II.3.4. Species diffusion coefficient

Diffusion coefficients of the gas mixture can be calculated as follows:

The diffusion coefficient D_j of neutral particle j in the background gases is calculated by first determining the separate binary diffusion coefficient D_{ij} using the following expression [22].

$$D_{ij} = \frac{3k_bT_{gas}\sqrt{2\pi k_bT_{gas}/m_{ij}}}{16\pi P_{tot}\sigma_{ij}^2\Omega_D(\mathrm{T}*)} \qquad \text{(I.6)}$$

Where:

P_i: the background species partial pressure i.

m_{ij}: the reduced mass, $m_{ij}=m_i m_j/(m_i+ m_j)$.

σ_{ij}: the binary collision, $\sigma_{ij}=(\sigma_i+\sigma_j)/2$.

$\varepsilon_{ij}=\sqrt{\varepsilon_i \varepsilon_j}$.

$T^*=T_{gas}/\varepsilon_{ij}(K)$.

ε_{ij} and T^* are the Lennard-Jones parameters.

K_b: Boltzmann constant.

$$\Omega_D(T*)=\frac{A}{T^{*B}}+\frac{C}{e^{D.T^{\mu}}}+\frac{E}{e^{F.T^*}}+\frac{G}{e^{H.T^*}} \quad \text{(II.7)}$$

Where: A = 1.06036, B = 0.15610, C = 0.19300, D = 0.47635, E = 1.03587, F = 1.52996, G = 1.76474, H = 3.89411.

The diffusion coefficient D_j of particle j in the background gas mixture i is then approximated, using Blancs law [23], by:

$$\frac{P_{tot}}{D_j}=\sum_i \frac{P_i}{D_{ij}} \quad \text{(II.8)}$$

P_{tot}:. Total pressure

The Lenard-Jones parameters σ and ε of different molecules and radicals are presented in table II.2.

Table II.2: Values of Lenard-Jones parameters σ and ε:

Particle	$\sigma_i(A^0)$	$\varepsilon_i(K)$	references
SiH_3	3.943	170.3	[24]
SiH_2	3.803	133.1	[24]
H_2	2.827	103	[24]
SiH_3O	3.69	417	[25]
H	2.5	30	[25]
SiH_2O	3.59	498	[25]
SiO	3.59	498	[25]
O_2	3.407	121.1	[25]
H_2O	2.673	535.21	[25]
SiH	3.662	95.8	[24]
SiO_2	3.59	498	[25]
OH	3.111	281.27	[25]
SiHO	3.59	498	[25]
O	3.064	57.91	[25]
SiH_4	4.084	207.6	[25]

II.4. Numerical model

In order to calculate numerically concentrations of neutral particles, we choose the Finite Differences Method (FDM). The FDM is based on the following steps:

- Discretization of the simulation scope.

- Approximation of the partial derivative by finite differences.

- Data initialization and determination of primary conditions and boundary conditions.

II.4.1. Discretization of the simulation scope and approximation of the partial derivative

We split the scope of study into numerous points j_{max}. We define space step by:

$$dz = \frac{zmax}{jmax-1} \quad \text{(II.9)}$$

For our numerical model, we use the Finite Differences Method (FDM). It's a method which depends on the approximation of partial derivative of Taylor's expansions of function.

Taylor's expansions according to the component z is [26]:

$$f(j \pm hz) = f_j \pm hz\left(\frac{\partial f}{\partial z}\right) + \frac{(hz^2)}{2!}\frac{\partial^2 f}{\partial^2 z} \pm \cdots \quad \text{(II.10)}$$

Partial derivative approximation of two ranks is:

$$\frac{\partial^2 f}{\partial z^2} = \frac{f(j-1)-2f(j)+f(j+1)}{\partial z^2} \quad \text{(II.11)}$$

II.4.2. Basic equation to calculate concentrations of particles

a) Basic equation

We apply the expressions of partial derivates of FDM, using equation (II.11) in (II.3) for a particle k. The numerical equation of concentration of each particle k takes the following form:

$$A_{j-1,j}C_{j-1}^k + A_{j,j}C_j^k + A_{j+1,j}C_{j+1}^k = B_j \; ; \;\; for\; j = 2, jmax-1 \quad \text{(II.12)}$$

Coefficients $A_{j-1,j}$, $A_{j,j}$, $A_{j+1,j}$ and B_j depend on parameters K_{reac}, D_k, C^k at different values j.

So we have a system of matrices equation of the form (A.X=B). For the numerical resolution, we apply the Gauss-Seidel iterative method. Equation II.12 presents the heart of our numerical program developed in Fortran 77 language.

For numerical calculation, the rate constant of the chemical reactions K_{rea} and the diffusion coefficient D_k are calculated using several data and parameters of the code.

c) Boundary conditions

For boundary conditions, we propose we propose a slow variation of the concentrations at the edges; that is to say:

$$\frac{\partial \ f}{\partial z} = 0 \qquad for\ z = 0\ and\ z = zmax \tag{II.13}$$

Or:

$$1.\,C_1^k + (-1.)C_2^k = 0\,;\ \ for{:}\ j = 1 \tag{II.14}$$

$$-1.\,C_{jmax-1}^k + 1.\,C_{jmax}^k = 0\,;\ \ for{:}\ j = jmax \tag{II.15}$$

II.4.3. Data initialization and determination of primary values

c) Data initialization

We take axial values, as function of z, of electron density $n_e(z)$, electron temperature $T_e(z)$ and gas temperature $T_{gaz}(z)$ from results of S. Tinck and A. Bogaerts (2012) [1].

d) Numerical initial values of neutral concentrations

For the calculation of the values of the concentrations $C_0^k(z)$ for the initialization of the data, we considered a simple approximation. We start by calculating approximate values of the concentrations of the products from the concentrations of the reactants. The calculation is done successively from the most important reactions.

The order of calculation is as follows:

- Initial concentrations of SiH_4 and O_2;
- Approximate concentrations of SiH_3, SiH_2,SiH, H, H_2;
- Correction of concentrations of SiH_4 and O_2;
- Approximate concentrations of OH, H_2, SiH_3O, SiH_2O and SiHO;
- Approximate concentrations of SiO, H_2O and SiO_2.

II.5. Diagram of the numerical calculation

We have developed a numerical program in Fortran language to calculate concentrations of neutral particles in an ICP reactor. The figure II.2 presents the diagram of the calculation.

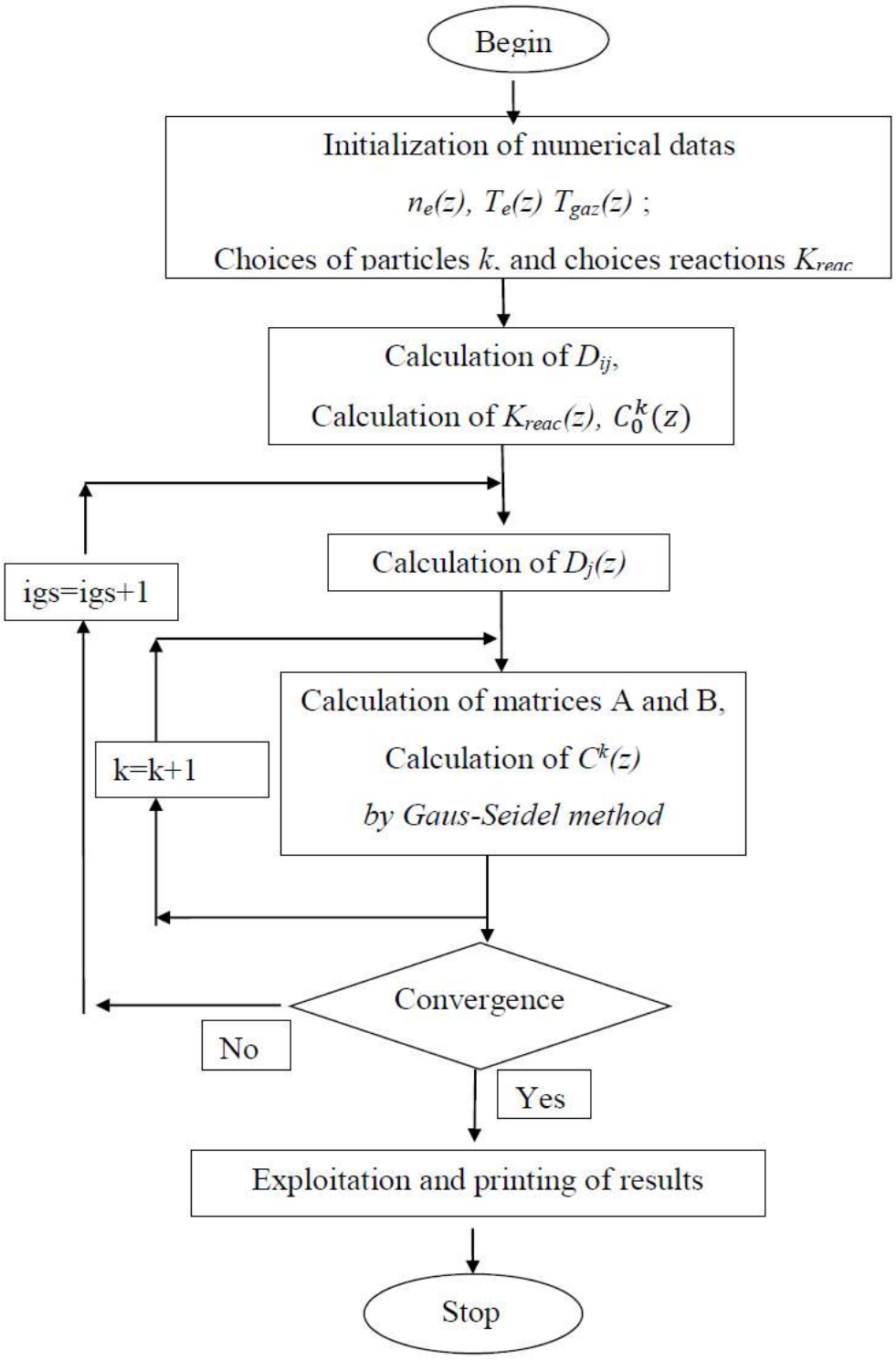

Figure II.2: Diagram to calculate concentration of neutral particles.

Chapter III:
Results and discussion

Chapter III: Results and discussion

III.1. Introduction

In this chapter we present the different results of the numerical modeling used for the calculation of the concentrations of molecules. The used data are taken from the work of S. Tinck and A. bogaerts. (2012) [1]. They did their study under specific conditions like the applied power is 13.56 MHz radio frequency for gas mixture of $SiH_4/O_2/Ar$ in Inductively Coupled Plasma.

For our study we use SiH_4/O_2 gas mixture in Inductively Coupled Plasma with applied power 13.56 MHz radio frequency. We select the dominant molecules which are: SiH_4, O_2, SiH_3, SiH_2, H_2, SiH_3O, H, SiH_2O, SiO, H_2O, SiH, SiO_2, OH, SiHO, O.

III.2. Electron density, electron temperature and gas temperature:

We use the experimental values of electron density, electron temperature and gas temperature according to the z axis with r=0. We proceed in three steps:

a. First, from two dimensional (2D) distribution function, we take the mean value of the function for each interval (j_i, j_{i+1}).

b. In the second step, between two successive intervals, the function takes the average value between intervals (equations III.1 and III.2).

$$\tan\alpha = \frac{f(j+1)-f(j)}{z(j+1)-z(j)} = \frac{f_2(j_2)-f(j)}{z_2(j_2)-z(j)} \qquad \text{(III.1)}$$

$$f(j) = f_2(j_2) - \frac{f(j+1)-f(j)}{z(j+1)-z(j)}\,(z_2(j_2)-z(j)) \qquad \text{(III.2)}$$

c. In the third step, we construct the continuous function f(z). The function has a constant value in each interval and it has a linear variation between two successive intervals.

III.2.1. Electron density

The figure III.1 presents the 2D distribution of electron density in the reactor as function of cylindrical coordinates (r,z) [1]. The figure III.2 presents the curve corresponding to the first and second steps (electron density in intervals). The figure III.3 presents the continuous function f(z) of electron density $n_e(z)=f(z)$, for r=0, corresponding to third step.

The choice of a continuous function is important for the resolution of numerical equations.

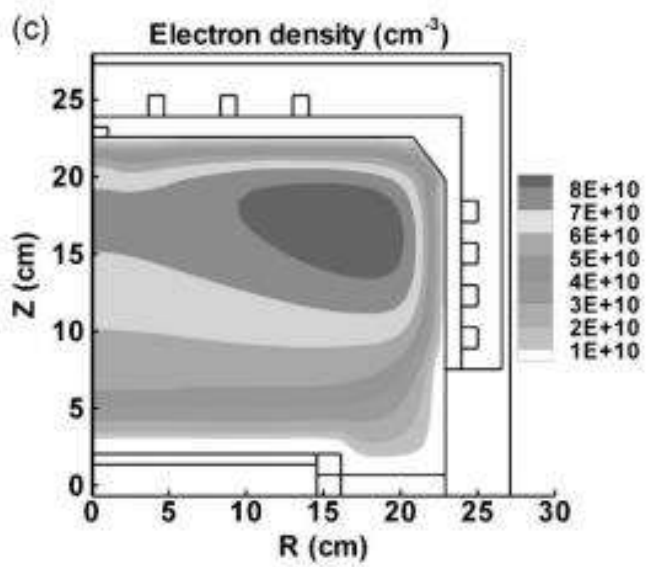

Figure III.1: 2D Distribution of electron density in the reactor [1].

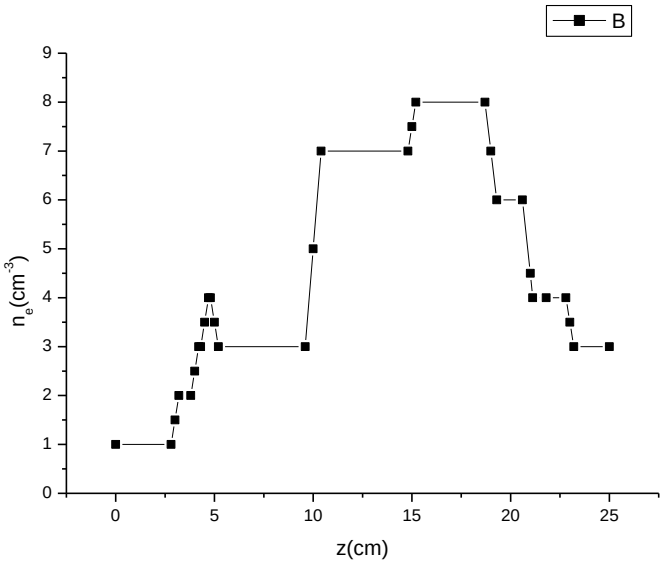

Figure III 2: Curve of axial electron density as function of z.

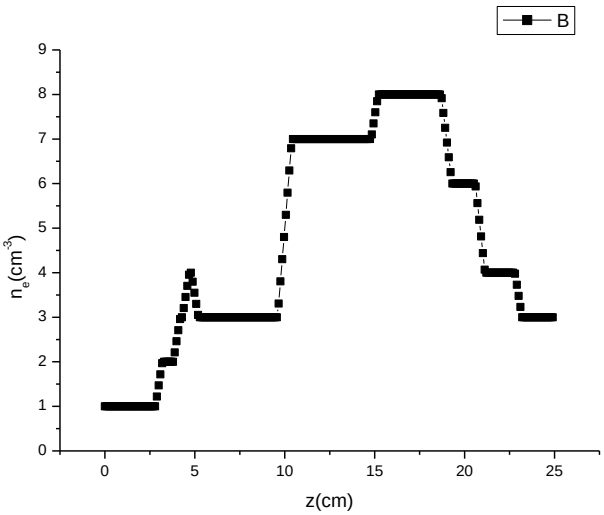

Figure: III 3: Continuous curve of axial electron density as function of z.

III.2.2. Electron temperature

Same as last section, the figure III.4 presents the 2D distribution of electron temperature in the reactor as function of cylindrical coordinates (r,z) [1]. The figure III.5 presents the curve corresponding to the first and second steps (electron temperature in intervals). The figure III.6 presents the continuous function f(z) of electron temperature $T_e(z)=f(z)$, for r=0, corresponding to third step.

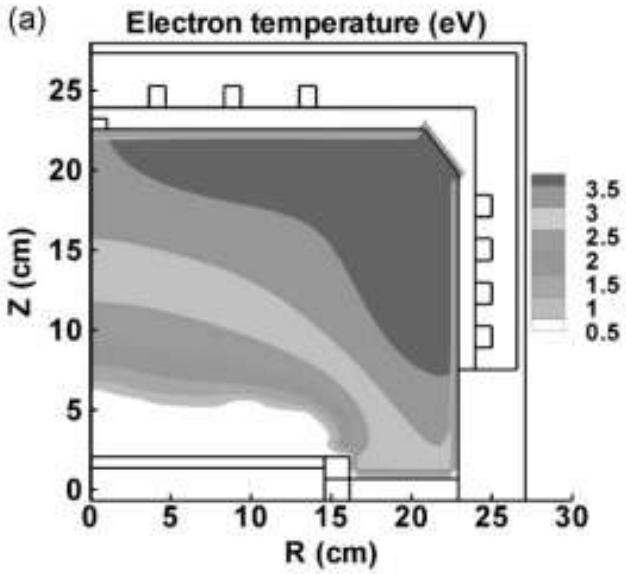

Figure III.4: 2D Distribution of electron temperature in the reactor [1].

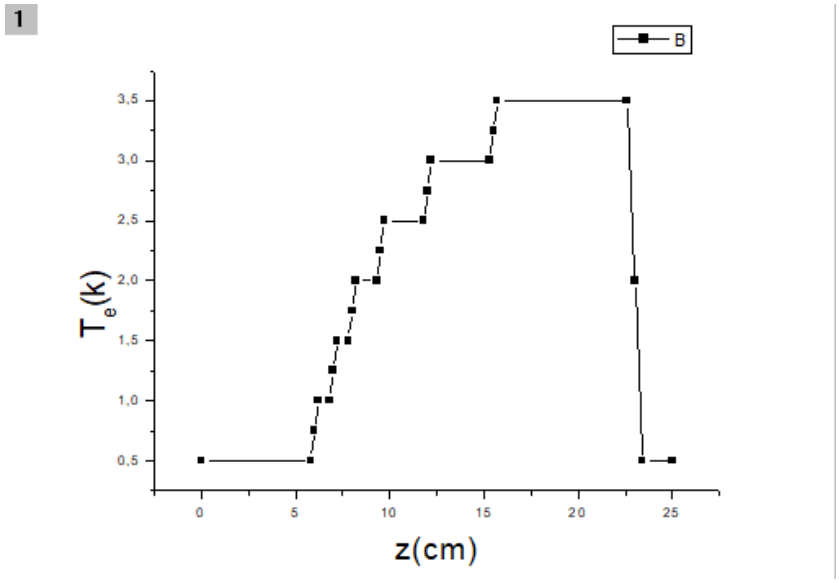

Figure III 5: Curve of electrons temperature as function of z.

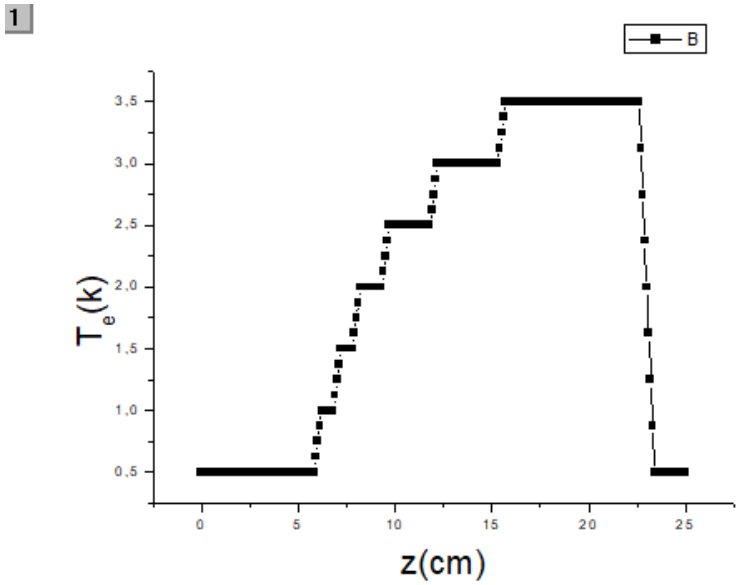

Figure III.6: Continuous curve of electrons temperature as function of z.

III.2.3. Gas temperature

Same as last two sections, the figure III.7 presents the 2D distribution of gas temperature in the reactor as function of cylindrical coordinates (r,z) [1]. The figure III.8 presents the curve corresponding to the first and second steps (gas temperature in intervals). The figure III.9 presents the continuous function f(z) of gas temperature $T_{gas}(z)=f(z)$, for r=0, corresponding to third step.

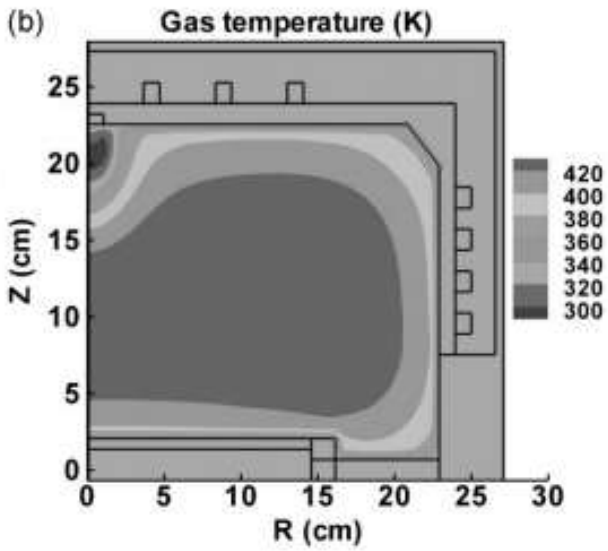

Figure III.7: 2D Distribution of gas temperature in the reactor.

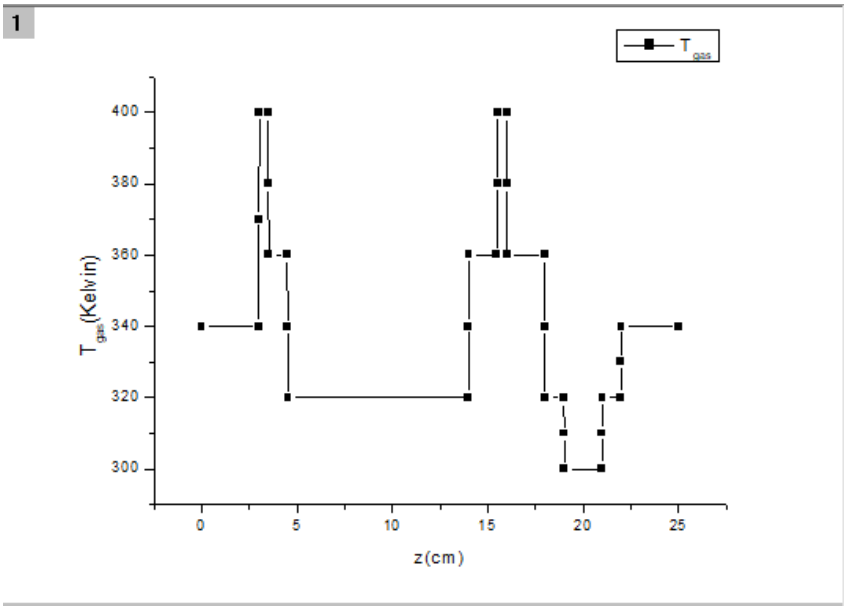

Figure III.8: Curve of gas temperature as function of z.

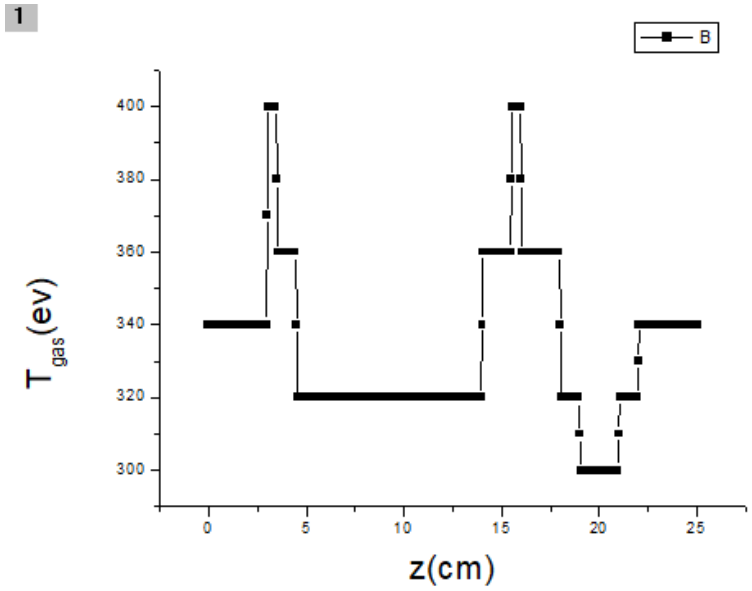

Figure III.9: Continuous curve of gas temperature as a function of z.

III.3. Variation of rate constant of chemical reactions with temperature

In this section we present variation of rate constant of some chemical reactions with temperature T and with gas temperature in the reactor.

We can see that the rate constants are different from each other as for rate number 31 is higher than the rate number 28 where their values are constants no matter how the temperature changes. While the rate number 30 is higher than both of them and increases with temperature T.

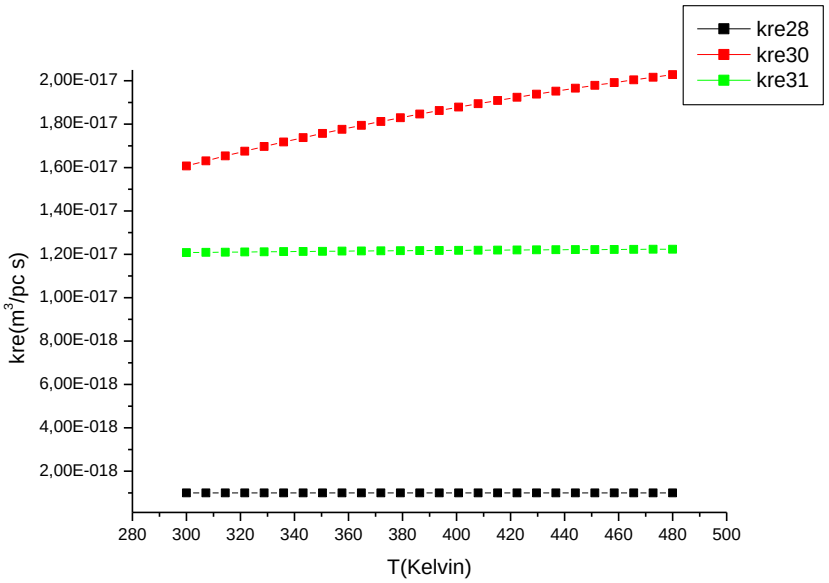

Figure III.10: Variation of rate constant of chemical reactions number 28, 30 and 31 as function of temperature T.

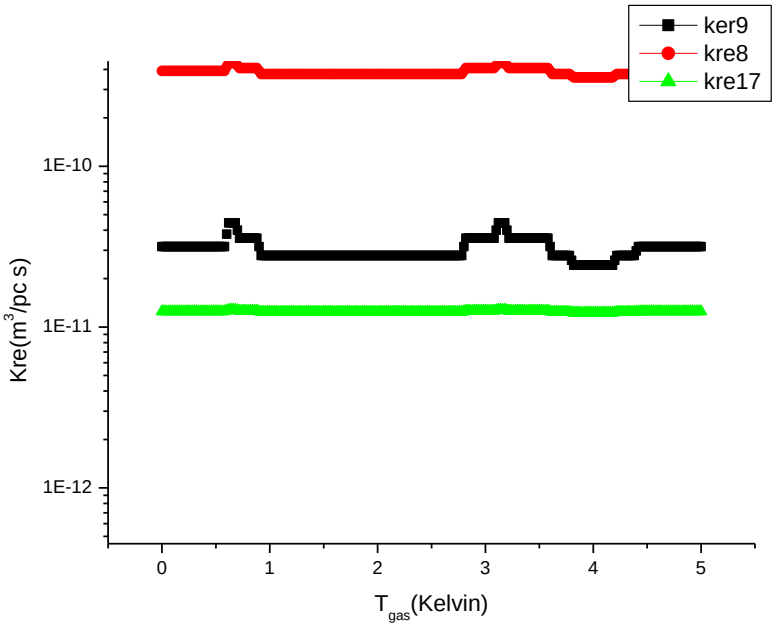

Figure III.11: Variation of rate constants number 9, 8 and 17 of chemical reactions.

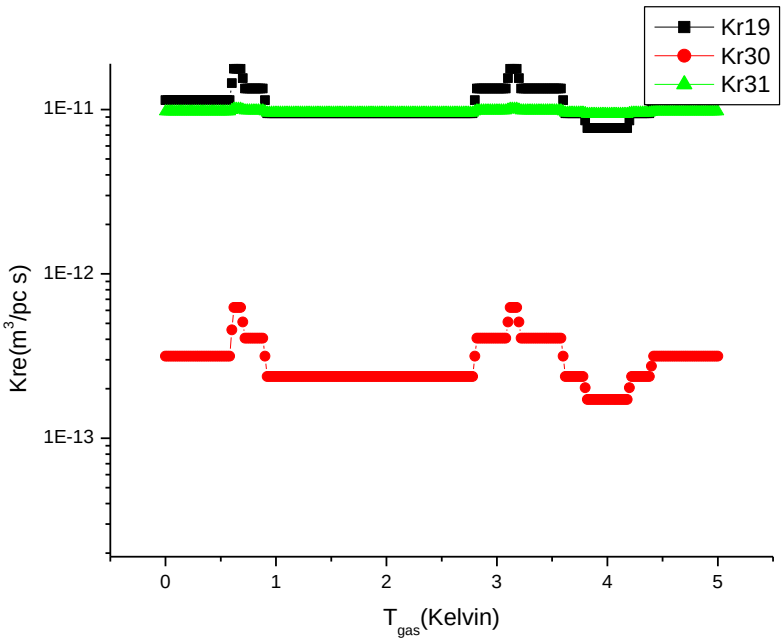

Figure III.12: Variation of rate constants number 19, 30 and 31 of chemical reactions.

In figure III.11 and figure III.12, we present the variation of rate constants of different chemical reaction (K_{reac} = 9, 8, 17, 19, 30, 31) as function of gas temperature T_{gas} in reactor. We can see that some rate are pratically constans

We can observe that the variation of the rate constants are not different from each other. For the rate for number 17 and 31, they are constant; the rate for the number 8, it has a small variation with the increase of the gas temperatue.

The rates for number 9 and 19, they have almost the same variation.

III.4. Determination of initial values of particles concentration C_0^k

We use the steps noted on section II.4.3 to calculate values of the concentrations $C_0^k(z)$ for the initialization of the data. The figures III.13 and III.14 show these initial concentrations for some neutral particles (molecules and radicals) for conditions of the reactor $T_{gaz}(z)$, $T_e(z)$ and $N_e(z)$.

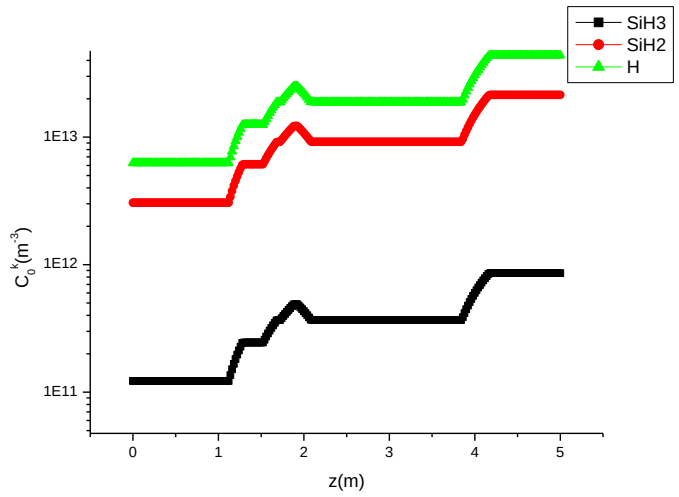

Figure III.13: Initial concentrations of particles SiH_3 SiH_2 and H as function of position z.

The initial concentrations of SiH_3 SiH_2 and H have the same shape of change but their values are different from each other. They stay constant at the scope from 0 meter to 1 meter while from 1 meter to 1.8 they increase with the increase of position z then they decrease. The scope of 2 meter to 4 meter they stay constant with the change of position z then they increase again and stay constant from 4.25 meter to 5 meter.

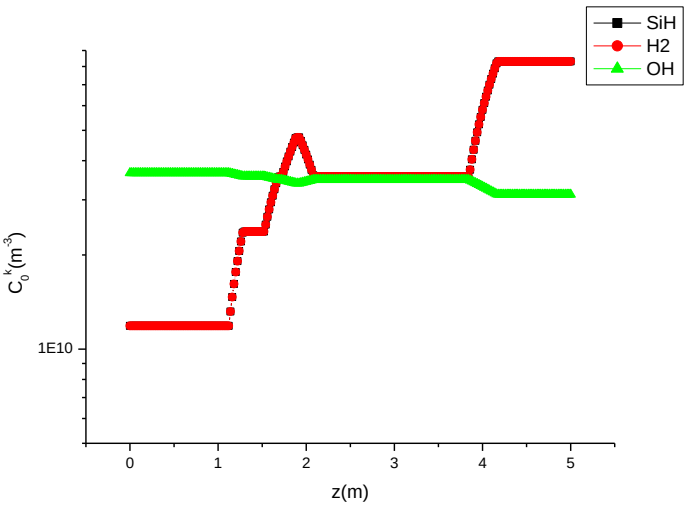

Figure III.14: Initial concentrations of particles SiH and H_2 as function of position z.

We can see that the initial concentrations of SiH and H_2 are equal at the scope 0 meter-1 meter they are constant with position z. while from

1meter to 2 meter they increase until they reach a higher point then they decrease and stay constant for the scope of (2.2 meter to 3.8 meter). At the position 3.8 meter they increase until reaching a specific value and stay constant.

The initial concentration of OH is almost constant for all position z.

III.5. Concentrations of neutral particles

Figures from III.15 to III.21 present the calculated concentrations of neutral particules. We have taken for calculation z_{max}=5cm (instead of z_{max}=25cm) and the same variations for $T_{gaz}(z)$, $T_e(z)$ and $N_e(z)$ approximated in section III.2..

The curves of SiH_3, SiH_2 and H_2 have the same shape; this behavior is related to chemical reactions number 1, 2 and 3.. The curves of SiH and H have the same shape too.

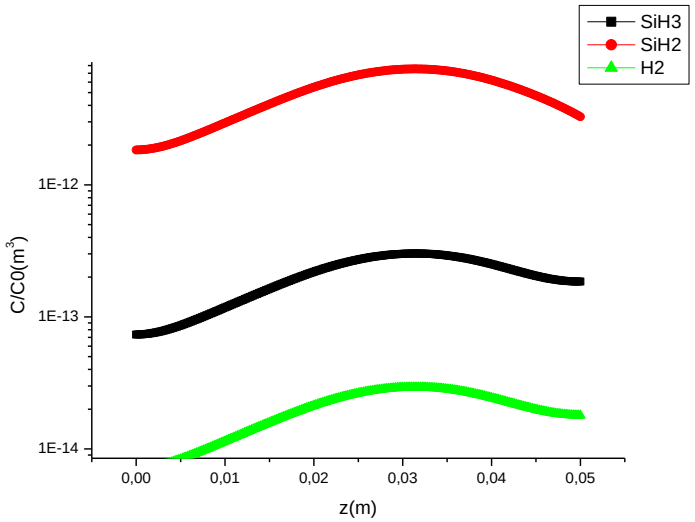

Figure III.15: Concentration of particles SiH_3, SiH_2 and H_2 as function of position z.

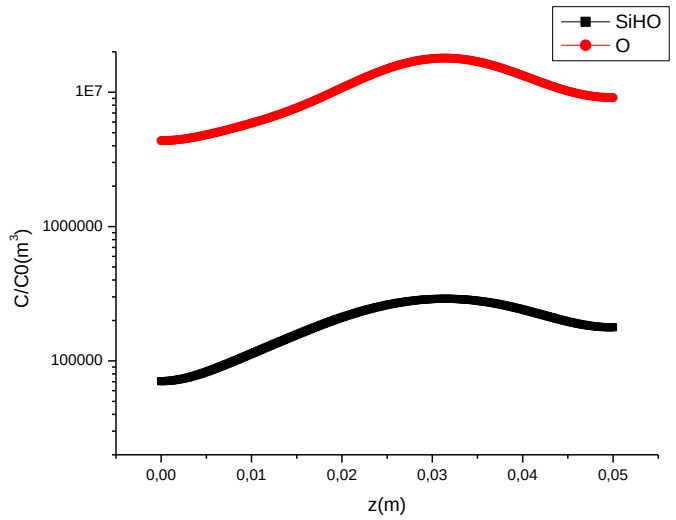

Figure III.16: Concentration of particles SiHO and O as function of position z.

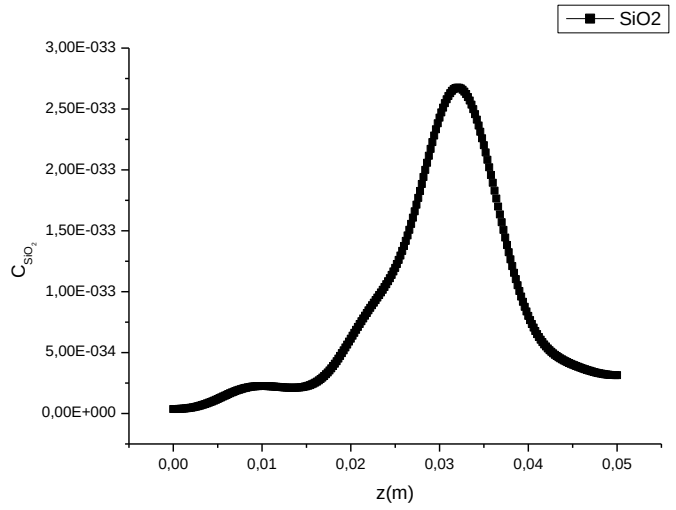

Figure III.17: Concentration of particles of SiO_2 as function of position z.

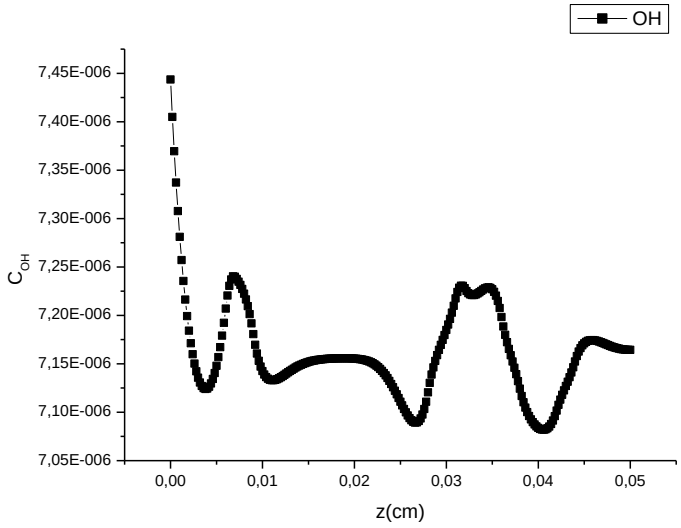

Figure III.18: Concentration of particles of OH as function of position z.

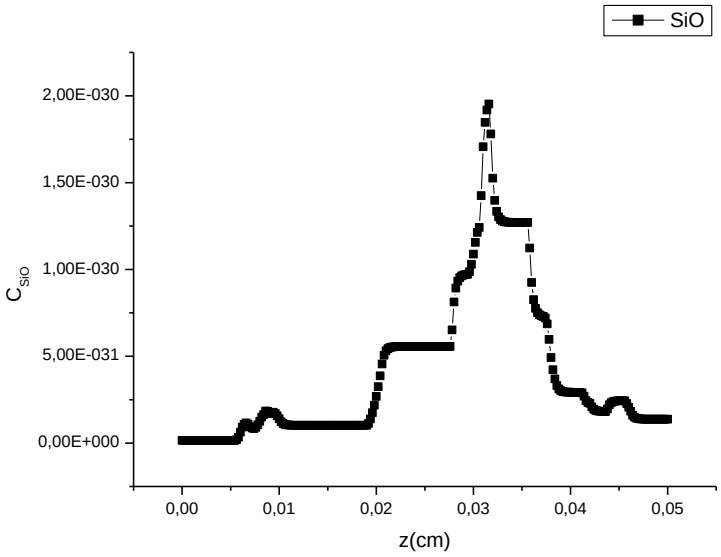

Figure III.19: Concentration of particles of SiO as function of position z.

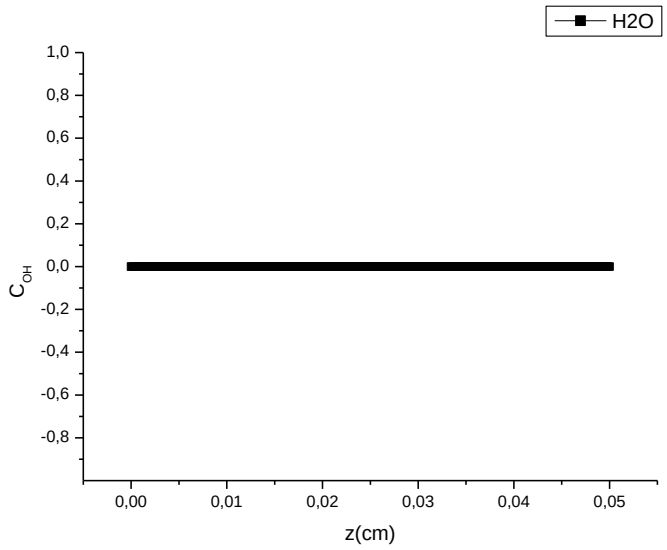

Figure III.20: Concentration of particles of H_2O as function of position z.

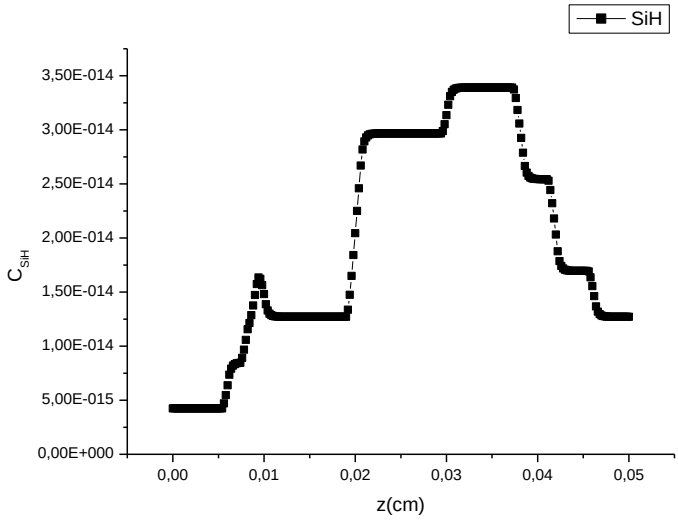

Figure III.21: Concentration of particles of SiH as function of position z.

III.6. Applications of results

First application of our calculation is the local pressure in reactor. We can calculate local partial pressure and total partial pressure in the reactor.

Local partial pressure of species k is:

$$P_k(z)=C_k(z).R.T_{gaz}(z)$$

Local total pressure of gas is:

$$P_{tot}(z)=\text{Sum}\ (P_k(z))= P_{k=1}(z)+ P_{k=2}(z)+\ldots.+ P_{k=15}(z)$$

A second application of the calculation is the estimation of the growth rate near the substrate. The knowledge of concentrations of radicals near the substrate, their temperatures and their probabilities of reaction with surface will be a good tool for the calculation.

General conclusion and perspectives

General conclusion and perspectives

Thin films are used widely in several fields like the fabrication of solar cells and the microelectronics. Deposition of these thin films can be obtained by two main techniques (CVD) and (PVD).

The silicon is one of the most used materials for the deposition because it facilitates the growth of thin films.

In this work we were interested in the study of a gas mixture of SiH_4/O_2 in Inductively Coupled Plasma (ICP). A radio frequency power is applied in the reactor. The initial proposals are 54% of SiH_4 and 46% of O_2.

We took 38 chemical reactions of the most 15 dominant neutral particles which are: SiH_4, O_2, SiH_3, SiH_2, H_2, SiH_3O, H, SiH_2O, SiO, H_2O, SiH, SiO_2, OH, SiHO, O.

In order to calculate the concentrations of different particles we suggested the resolution of the continuity equation. We took the system in one dimension and stationary system. The rate constants vary with position z.

For the numerical modeling we applied Finite Differences Method (FDM) and iterative algorithm of Gauss-Seidel.

We compared our results with S. Tinck and A. Bogaerts results.

We suggested the following perspectives:

-Study of more particles for example ions and electrons.
-Study of fluid model in 2 or 3 dimensions.
-Study of the magnetic field inside the reactor.

References

References

[1] S. Tinck and A. Bogaerts; “Modeling SiH_4/O_2/Ar Inductively Coupled Plasmas Used for Filling of Microtrenches in Shallow Trench Isolation (STI)”; Plasma Processes and Polymers, Vol. 9, no. 5, pp 1-18, 2012.

[2] L. Tonks and I. Langmuir; ”Oscillations in Ionized Gases”; Phys. Rev., Vol. 33, 195, 1929.

[3] G. Fischer; “Reactive ion etching of crystalline silicon plasma nanotexturing of Silicon for photovoltaic applications: Tailoring plasma-surface interactions for improved light management plasma physics; Doctoral thesis; Université Paris Saclay, 2018.

[4] D. R. Nicholson; “Introduction to plasma theory”; John Wiley & Sons, New York, 1983, XII, 292 pp.

[5] L. Benmebrouk; "Etude des Spectres d’émission d’ions de déposition sur couches minces"; Mémoire de Magister, Université de Kasdi Merbah Ouargla, 2003.

[6] Michael C. Kelley;”The earth’s electric field”; Elsevier, pp 187-214 USA.

[7] F. J. Yusta, M. L. Hitchman and S. H. Shamlian; "CVD preparation and characterization of tin dioxide films for electrochemical applications"; J. Mater. Chem., Vol. 7, p1421, 1997.

[8] B. H. Ibrahim; "The deposition of multilayer and gradient index thin films by Matrix Distributed Electron Cyclotron Resonance Plasma Enhanced Chemical Vapor Deposition MDECR-PECVD"; Doctoral thesis École Polytechnique, 2007

[9] ز.بلة؛ "الدراسة التشخيصية بالمحاكاة العددية لمسبار كهربائي ساكن في رش مهبطي"؛ مذكرة ماجستير؛ جامعة قاصدي مرباح ورقلة 2007 .

[10] O. Babahani; "Cours physique des surfaces (chap. I); Master Physique des Rayonnements (2017-2018).

[11] H. C. Lee; ”Review of inductively coupled plasmas: Nano-applications and bistable hysteresis”; Appl. Phys. Rev., Vol. 5, no. 1, 011108, 2018.

[12] T. Okumura; ”Inductively Coupled Plasma sources and applications” ; Physics Research International; Vol. 2010, Article ID 164249, pages 14, 2010.

[13] Denise C. Marra and Erik A. Edelberg; ”Silicon hydride composition of plasma-deposited hydrogenated amorphous and nanocrystalline silicon films and surfaces”; J. Vac. Sci. Technol. A, Vol. 16, no. 6, pp 3200-3202, 1998.

[14] C. R. Gorla, S. Liang, G. S. Tompa, W. E. Mayo and Y. Lu; “Silicon and germanium nanoparticle formation in an inductively coupled plasma reactor”; Silicon and germanium nanoparticle formation, Vol. A 15, no. 3, pp 860-861, 1997.

[15] G. J. Nienhuisa and W. J. Goedheer; "A self-consistent fluid model for radio-f requency discharges in SiH4–H2 compared to experiments"; Journal of applied physics, Vol. 82, no. 5, pp 2060-2071, 1997.

[16] C. Jia, J. Linhong , Z. Yu and S. Yixiang, ”Fluid model of inductively coupled plasma etcher based on COMSOL”; Journal of Semiconductors, Vol. 31, No. 3; pp: 03004-2, 2010.

[17] Yu. E. Gorbachev; ”Effect of oligomers on the growth of amorphous silicon films in a PECVD reactor”; Technical Physics, Vol. 51, No. 6, pp. 733–733, 2006.

[18] M. J. Kushner; ”A model for the discharge kinetics and plasma chemistry during plasma enhanced chemical vapor deposition of amorphous silicon”; J. Appl. Phys., Vol. 63, 2532, 1988.

[19] K. De Bleecker, D. Herrebout, A. Bogaerts, R. Gijbels and P. Descamps; ” One-dimensional modelling of a capacitively coupled rf plasma in silane/helium, including small concentrations of O_2 and N_2 ”; J. Phys. D: Appl. Phys. Vol. 36, No. 15, 2003.

[20] UMIST RATE12 astrochemistry.net, http://udfa.ajmarkwick.net/index.php ; consulted on: 26/05/2021.

[21] NIST, Chemical Kinetics Database, http://kinetics.nist.gov/kinetics/index.jsp ; consulted on: 24/05/2021.

[22] H. ElWelly, H. Abdel Mohsen and F. ElTokhi; “Numerical study of particles generation and flow in SiH_4/H_2 discharge”; The Egyptian Int. J. of Eng. Sci. and Technology, Vol. 16, N° 1, pp 92-93, 2013.

[23] D. Herrebout, A. Bogaerts, M. Yan and R. Gijbels; “One-dimensional fluid model for an RF methane plasma of interest in deposition of diamond-like carbon layers”; Journal of Applied Physics"; Vol. 90, pp 570-578 2001.

[24] R. J. Kee, G. Dixon-Lewis, J. Warnatz, M. E. Coltrin, J. A. Miller, H. K. Moffat; ”Transport: a software package for the evaluation of gas-phase, multicomponent transport properties ”; Chemkin Collection, 1999.

[25] W. Z. Jia, R. Q. Liu, X. F. Wang, X. M. Liu, Y. H. Song and Y. N. Wang; ”Two-dimensional fluid simulation of a radio frequency capacitively coupled plasma in $SiH_4/N_2/O_2$”; Physics of Plasmas, Vol. 25, No. 9, pp: 093501-1-093501-17, 2003.

[26] M. Sibonyet and J. Claude Mardon; "Approximations et équations différentielles"; Hermann 1982.

[27] F. Khelfaoui and O. Babahani; ”How to use the Monte Carlo Simulation Technique Application: A study of the gas phase during thin film deposition”; Book Chapter; Academic Editor : Pooneh Saidi; in intechopen; August 2019. DOI: 10.5772/intechopen.88559.

[28] C. S. Corr, S. Gomez, and W. G. Graham; “Discharge kinetics of inductively coupled oxygen plasmas: experiment and model”; Plasma Sources Science and Technology, Vol. 21(5), 055024, 2012.

ملخص:

يهتم عملنا بحساب تراكيز مختلف العناصر لخليط غاز SiH_4/O_2 المستعمل في توضع الطبقات الرقيقة بواسطة بلازما مقترنة بالحث (ICP) و بالاعتماد على المعطيات الخاصة بأعمال S. Tinck and A. Bogaerts لكل من (T_e, T_{gas}, n_e). كما قمنا بإعداد برنامج عددي بلغة Fortran77 لحساب معامل الإنتشار و ثوابت التفاعلات الكيميائية و التراكيز لمختلف العناصر. يعتمد برنامجنا على نموذج الموائع (معادلة الاستمرارية) و طريقة الفروق المنتهية و خوارزمية غوص صايدل التكرارية. تحصلنا على تراكيز مختلف العناصر و التي تتوافق مع نتائج S. Tinck and A. Bogaerts.

الكلمات المفتاحية: SiH_4/O_2، ICP، تراكيز، معامل الإنتشار، ثوابت التفاعلات الكيميائية، نموذج الموائع، طريقة الفروق المنتهية، خوارزمية غوص صايدل.

Abstract:

In our work, we interested in calculation of concentrations of different neutral particles, molecules and radicals, for a gas mixture of SiH_4/H_2 used in thin films deposition by Inductively Coupled Plasma (ICP) and based on the data of S. Tinck and A. Bogaerts works for T_e,T_{gas}, and n_e. We developed a numerical code in Fortran 77 language for the calculation of diffusion coefficient, rate constants of chemical reactions and concentrations for different particles. The code depend on the fluid model (the continuity equation), Finite Differences Method and algorithm iterative of Gauss-Seidel. We obtained the different concentrations of particles which correspond with the results of S. Tinck and A. Bogaerts.

Keywords: SiH_4/O_2, (ICP), concentrations, diffusion coefficient, rate constants, fluid model, Finite Differences Method, algorithm of Gauss-Seidel.

Résumé:

Notre travail s'intéresse au calcul des concentrations de différentes particules neutres, molécules et radicaux, pour un mélange gazeux $SiH_4/0_2$ utilisé pour la déposition des couches minces dans un Plasma à Couplage Inductif (ICP). Nous avons utilisé les données des travaux de S. Tinck and A. Bogaerts pour T_e, T_{gas} and n_e. Nous avons élaboré un programme numérique en langage Fortran 77 pour le calcul des coefficients de diffusion, les constantes des réactions chimiques et les concentrations de différentes molécules. Le programme se base sur le modèle fluide (équation de continuité) la Méthode des Différences Finies et l'algorithme itératif de Gauss-Seidel. Nous avons obtenu les différentes concentrations des molécules ; elles correspondent aux résultats de S. Tinck and A. Bogaerts.

Mots clés : SiH_4/O_2, ICP, concentrations, coefficients de diffusion, constantes de réactions, modèle fluide, Méthode des Différences Finies, Gauss-Seidel algorithme.